DOI: 10.15415/jnp.2017.42030

# Possible Alpha and $^{14}$C Cluster Emission From Hyper Radium Nuclei in The Mass Region A = 202−235

K. P. SANTHOSH AND C. NITHYA

School of Pure and Applied Physics, Kannur University, Swami Anandatheertha Campus, Payyanur 670327, INDIA

**Email: drkpsanthosh@gmail.com**

Received: August 24, 2016| Revised: December 13, 2016| Accepted: January 09, 2017

Published online: February 06, 2017



**Abstract** The possibilities for the emission of $^{4}$He and $^{14}$C clusters from hyper $^{202-235}_{\Lambda}Ra$ are studied using our Coulomb and proximity potential model (CPPM) by including the lambda−nucleus potential. The predicted half lives show that hyper $^{202-231}_{\Lambda}Ra$ nuclei are unstable against $^{4}He$ emission and $^{14}C$ emission from $^{217-229}_{\Lambda}Ra$ are favorable for measurement. Our study also show that hyper $^{202-235}_{\Lambda}Ra$ are stable against hyper $^{4}_{\Lambda}He$ and $^{14}_{\Lambda}C$ emission. The role of neutron shell closure (N = 126) in $^{213}_{\Lambda}Rn$ daughter and role of proton and neutron shell closure (Z = 82, N = 126) in $^{209}_{\Lambda}Pb$ daughter are also revealed. As hyper nuclei decays to normal nuclei by mesonic/non−mesonic decay and since most of the predicted half lives for $^{4}He$ and $^{14}C$ emission from normal Ra nuclei are favorable for measurement, we presume that alpha and $^{14}C$ cluster emission from hyper Ra nuclei can be detected in laboratory in a cascade (two−step) process.

## 1. INTRODUCTION

The existence of nuclei containing hyperons is one of the interesting phenomena in nuclear physics. The characteristic feature of the hyperon is that it is free from the Pauli Exclusion Principle, and thus it can deeply penetrate into the nuclear interior. A hyperon may modify several properties of nuclei, such as

Journal of Nuclear Physics, Material Sciences, Radiation and Applications
Vol-4, No-2,
Feburary 2017
pp. 337-353



CHITKARA UNIVERSITY

nuclear size [1, 2], the density distribution [3], deformation properties [4, 5], the neutron/proton drip−line [6, 7, 8], and fission barrier [9, 10]. The study on hyper nuclei will improve our knowledge on the fundamental hyperon−nucleon interaction.

The lifetime of hyperons bound in hyper nuclei is affected by the nuclear environment. The decay of free $\Lambda$−hyperon is purely mesonic, $\Lambda \rightarrow N + \pi$ , but in heavy hyper nuclei mesonic decay is negligible and the total decay width is due to the non−mesonic decay channels. Ohm et al [11] have shown the lifetime of the hyperon in heavy hyper nuclei to be roughly of the same magnitude as for the free $\Lambda$−hyperon decay and also experimentally shown that (p,K) reaction is an effective method to produce heavy hyper nuclei with large cross sections (~ 150 mb) even at the sub threshold bombarding energy of $T_p = 51.5$ GeV.

Production of hyper nuclei [12] can be achieved through "strangeness−exchange reaction" which requires the injection of $\pi^+$ or $K^-$ beams on fixed targets (see [13] and references therein) and also electron beams on fixed targets [14, 15]. When a $K^-$ stops inside a nucleus, a neutron is replaced by a $\Lambda$ hyperon with the emission of a pion. By precisely studying momentum of the outgoing pions both the binding energy and the formation probability [16] of the hyper nuclei can be measured.

In the present paper we have made an attempt to study how hyper nuclei behave against alpha and heavy cluster emission, by comparing the tunneling probability/half life of alpha and heavy cluster in hyper nuclei and in non−strange normal nuclei. Alpha decay is one of the main decay modes in heavy nuclei and was observed by Rutherford [17, 18] a century ago. Alpha decay was first interpreted as quantum mechanical tunneling through the potential barrier by Gamow [19] and independently by Gurney and Condon [20] in 1928. There are many effective theoretical approaches that have been used to describe alpha decay, such as Generalized Liquid Drop Model (GLDM) [21], Generalized Density dependent Cluster Model (GDDCM) [22], Unified Model for Alpha Decay and Alpha Capture (UMADAC) [23], and Coulomb and Proximity Potential Model (CPPM) [24], and all of them have been successful in reproducing the experimental data.

Cluster radioactivity, the emission of particle heavier than alpha particle was first predicted by Sandulescu et al. [25] in 1980 and such decays were first observed experimentally by Rose and Jones [26] in 1984 in the radioactive decay of $^{223}Ra$ by the emission of $^{14}C$. The cluster decay process has been studied extensively using different theoretical models with different realistic nuclear interaction potentials. Generally, two kinds of models are used for explaining the observed decay modes and for predicting the possible decays. One of them

is the super asymmetric fission model [27–30] in which the nucleus is assumed to be deformed continuously as it penetrates the nuclear barrier and reaches the scission configuration after running down the Coulomb barrier. The other one is the Pre−formed cluster model [31–33] in which alpha particle and the heavy clusters are assumed to be pre−born in the parent nucleus, before they could penetrate the barrier.

Using the Coulomb and Proximity Potential Model, by including the lambda−nucleus potential, we have studied $^{4}He$ and $^{14}C$ clusters emission from hyper $^{202-235}_{\Lambda}Ra$ and non−strange $^{202-235}Ra$ nuclei to find the most promising hyper nuclei which are most favorable for emission. We have also studied the possibility for the emission of hyper $^{4}_{\Lambda}He$ and $^{14}_{\Lambda}C$ cluster from these parent nuclei. We would like to mention recently we have performed a study [34] on the probability for the emission of $^{4}He$ and $^{14}C$ cluster from hyper $^{207-234}_{\Lambda}Ac$ and non−strange normal $^{207-234}_{\Lambda}Ac$ nuclei. The Coulomb and Proximity Potential Model [24, 30] have been successful in studying alpha and cluster radioactivity in various mass regions of the nuclear chart. In this model, the interacting barrier for the post scission region is taken as the sum of Coulomb and proximity potential and for the overlap region a simple power law interpolation is used.

The formalism of the Coulomb and Proximity Potential Model (CPPM) is presented in Sec. 2. The result and discussion on the decay of hyper $^{202-235}_{\Lambda}Ra$ and non−strange $^{202\text{-}235}Ra$ nuclei are given in Sec. 3, and, in Sec. 4, we summarize the entire work.

## 2. THE COULOMB AND PROXIMITY POTENTIAL MODEL (CPPM)

In the Coulomb and proximity potential model (CPPM), the potential energy barrier is taken as the sum of Coulomb potential, proximity potential and centrifugal potential for the touching configuration and for the separated fragments. For the pre−scission (overlap) region, simple power law interpolation as done by Shi and Swiatecki [35] is used. The inclusion of proximity potential reduces the height of the potential barrier, which closely agrees with the experimental result. The proximity potential was first used by Shi and Swiatecki [35] in an empirical manner and has been quite extensively used by Gupta et al., [33] in the Preformed Cluster Model (PCM). R K Puri et al., [36, 37] has been using different versions of proximity potential for studying fusion cross section of different target−projectile combinations. In our model, the contribution of both internal and external part of the barrier is considered for the penetrability calculation. In present model assault frequency, $\nu$ is calculated for each parent−cluster combination which is associated with

vibration energy. For example in the case of alpha emission from $^{222}$Ra, ν is obtained as 3.068 x $10^{20}$ $s^{-1}$ and for $^{223}$Ra, ν is 2.746 x $10^{20}$ $s^{-1}$. For $^{14}$C emission from $^{222}$Ra, ν is 9.064 x $10^{20}$ $s^{-1}$ and for $^{223}$Ra, ν is calculated as 1.131 x $10^{21}$ $s^{-1}$. But Shi and Swiatecki [38] get empirically, the unrealistic values for the assault frequency $\nu$ as $10^{22}$ for even−A parents and $10^{20}$ for odd−A parents. The interacting potential barrier for two spherical nuclei is given by

$$V = \frac{Z_1 Z_2 e^2}{r} + V_p(z) + \frac{\hbar^2 \ell(\ell+1)}{2\mu r^2} \quad \text{for } z > 0 \tag{1}$$

Here $Z_1$ and $Z_2$ are the atomic numbers of the daughter and emitted cluster, 'z' is the distance between the near surfaces of the fragments, 'r' is the distance between fragment centres, $\ell$ represents the angular momentum, $\mu$ the reduced mass, $V_P$ is the proximity potential given by Blocki *et al*., [39] as

$$V_p(z) = 4\pi\gamma b\left[\frac{C_1 C_2}{(C_1 + C_2)}\right]\Phi\left(\frac{z}{b}\right) \tag{2}$$

With the nuclear surface tension coefficient,

$$\gamma = 0.9517[1 - 1.7826(N-Z)^2 / A^2] \quad \text{MeV/fm}^2 \tag{3}$$

where N, Z and A represent the neutron, proton and mass number of the parent, $\Phi$ represents the universal proximity potential [40] given as

$$\Phi(\varepsilon) = -4.41e^{-\varepsilon/0.7176} \quad \text{for } \varepsilon \geq 1.9475 \tag{4}$$

$$\Phi(\varepsilon) = -1.7817 + 0.9270\varepsilon + 0.0169\varepsilon^2 - 0.05148\varepsilon^3 \quad \text{for } 0 \leq \varepsilon \leq 1.9475 \tag{5}$$

With $\varepsilon = z/b$, where the width (diffuseness) of the nuclear surface $b \approx 1$ and Süsmann central radii $C_i$ of the fragments related to sharp radii $R_i$ is

$$C_i = R_i - \left(\frac{b^2}{R_i}\right) \tag{6}$$

For $R_i$ we use the semi empirical formula in terms of mass number $A_i$ as [39]

$$R_i = 1.28A_i^{1/3} - 0.76 + 0.8A_i^{-1/3} \tag{7}$$

The potential for the internal part (overlap region) of the barrier is given as

$$V = a_0\left(L - L_0\right)^n \qquad \text{for } z < 0 \tag{8}$$

where $L = z + 2C_1 + 2C_2$ and $L_0 = 2C$, the diameter of the parent nuclei. The constants $a_0$ and n are determined by the smooth matching of the two potentials at the touching point.

Using one dimensional WKB approximation, the barrier penetrability P is given as

$$\mathrm{P} = \exp\left\{-\frac{2}{\hbar}\int_a^b \sqrt{2\mu(V-Q)}dz\right\} \tag{9}$$

Here the mass parameter is replaced by $\mu = mA_1A_2 / A$, where m is the nucleon mass and $A_1$, $A_2$ are the mass numbers of daughter and emitted cluster respectively. The turning points "a" and "b" are determined from the equation, $V(a) = V(b) = Q$. The above integral can be evaluated numerically or analytically, and the half life time is given by

$$T_{1/2} = \left(\frac{\ln 2}{\lambda}\right) = \left(\frac{\ln 2}{\nu P}\right) \tag{10}$$

where, $\nu = \left(\frac{\omega}{2\pi}\right) = \left(\frac{2E_v}{h}\right)$ represent the number of assaults on the barrier per second and λ the decay constant. $E_v$ the empirical vibration energy is given as [41]

$$E_v = Q\left\{0.056 + 0.039\exp\left[\frac{(4-A_2)}{2.5}\right]\right\} \quad \text{for } A_2 \geq 4 \tag{11}$$

In the classical method, the α particle is assumed to move back and forth in the nucleus and the usual way of determining the assault frequency is through the expression given by $\nu = velocity / (2R)$, where $R$ is the radius of the parent nuclei. But the alpha particle has wave properties; therefore a quantum mechanical treatment is more accurate. Thus, assuming that the alpha particle vibrates in a harmonic oscillator potential with a frequency ω, which depends

on the vibration energy $E_V$, we can identify this frequency as the assault frequency $\nu$ given in eqns. (10)−(11).

## 3. RESULTS AND DISCUSSION

The half lives for the emission of $^{4}He$ and $^{14}C$ clusters from hyper $^{202-235}_{\Lambda}Ra$ and non−strange $^{202-235}Ra$ nuclei have been calculated using the Coulomb and proximity potential model (CPPM) by including the lambda−nucleus potential. The decay energy of the reaction is given as

$$Q = \Delta M - (\Delta M_1 + \Delta M_2) > 0 \tag{12}$$

Here $\Delta M$ ,$\Delta M_1, \Delta M_2$ are the mass excess of the parent, daughter and cluster respectively.

Hyper nucleus can be considered as the core of a normal nucleus plus the hyperons. The binding energy of the hyper nucleus can be written as

$$B(A,Z)_{hyper} = B(A-1,Z)_{core} + S_{\Lambda} \tag{13}$$

where $B(A\text{-}1, Z)_{core}$ is the binding energy of a hyper nucleus, $B(A-1, Z)_{core}$ is the binding energy of its non−strange core nucleus and $S_{\Lambda}$ is the $\Lambda$ −hyperon separation energy. For computing Q values experimental $\Lambda$ −hyperon separation energies are taken from Ref [42−47] and binding energies from latest mass tables of Wang et al [48]. The nuclei for which the experimental $\Lambda$ −hyperon separation energies are not available, binding energy formula reported by Samanta et al [49] is used to calculate hyperon separation energy. But to get better accuracy we used the formula which is obtained by least square regression to the experimental data given as

$$S_{\Lambda} = 0.036A + 18.90 \quad \text{for} \quad A \geq 50 \tag{14}$$

In Table 1 the computed Q values and logarithm of half lives for the decay of $^{4}He$ from hyper $^{202-235}_{\Lambda}Ra$ and non−strange normal $^{202-235}_{\Lambda}Ra$ nuclei are displayed. In the case of hyper nuclei, the half lives are computed by taking into account of the changes in both the decay Q value and interacting potential due to a $\Lambda$ −particle. To account for the changes in the potential due to a $\Lambda$ −particle, we have included the lambda−nucleus potential, $V_{\Lambda}$ in the expression for the interacting potential (eqn. 1) and is given by

$$V_{\Lambda} = \int \rho_{\Lambda}(r_1) V_{\Lambda N}(r_1 - r) d^3 r_1 \tag{15}$$

**Table 1**: Computed Q value and logarithm of half lives for the decay of $^{4}He$ from hyper $^{202-235}_{\Lambda}Ra$ and non−strange $^{202\text{-}235}Ra$ nuclei. $T_{1/2}$ is in second.

| Decay | Q Value (MeV) | $\log_{10}(T_{1/2})$ | Decay | Q Value (MeV) | $\log_{10}(T_{1/2})$ | |
|---|---|---|---|---|---|---|
| | | | | | Theory | Expt. [51] |
| $^{202}_{\Lambda}Ra \rightarrow {}^{4}He + {}^{198}_{\Lambda}Rn$ | 7.682 | −1.162 | $^{202}Ra \rightarrow {}^{4}He + {}^{198}Rn$ | 7.896 | −1.483 | |
| $^{203}_{\Lambda}Ra \rightarrow {}^{4}He + {}^{199}_{\Lambda}Rn$ | 7.663 | −1.117 | $^{203}Ra \rightarrow {}^{4}He + {}^{199}Rn$ | 7.745 | −0.988 | |
| $^{204}_{\Lambda}Ra \rightarrow {}^{4}He + {}^{200}_{\Lambda}Rn$ | 7.673 | −1.174 | $^{204}Ra \rightarrow {}^{4}He + {}^{200}Rn$ | 7.636 | −0.627 | |
| $^{205}_{\Lambda}Ra \rightarrow {}^{4}He + {}^{201}_{\Lambda}Rn$ | 7.492 | −0.547 | $^{205}Ra \rightarrow {}^{4}He + {}^{201}Rn$ | 7.485 | −0.104 | |
| $^{206}_{\Lambda}Ra \rightarrow {}^{4}He + {}^{202}_{\Lambda}Rn$ | 7.352 | −0.050 | $^{206}Ra \rightarrow {}^{4}He + {}^{202}Rn$ | 7.415 | 0.132 | |
| $^{207}_{\Lambda}Ra \rightarrow {}^{4}He + {}^{203}_{\Lambda}Rn$ | 7.272 | 0.232 | $^{207}Ra \rightarrow {}^{4}He + {}^{203}Rn$ | 7.274 | 0.642 | |
| $^{208}_{\Lambda}Ra \rightarrow {}^{4}He + {}^{204}_{\Lambda}Rn$ | 7.152 | 0.675 | $^{208}Ra \rightarrow {}^{4}He + {}^{204}Rn$ | 7.273 | 0.625 | |
| $^{209}_{\Lambda}Ra \rightarrow {}^{4}He + {}^{205}_{\Lambda}Rn$ | 7.132 | 0.733 | $^{209}Ra \rightarrow {}^{4}He + {}^{205}Rn$ | 7.135 | 1.139 | |
| $^{210}_{\Lambda}Ra \rightarrow {}^{4}He + {}^{206}_{\Lambda}Rn$ | 7.002 | 1.231 | $^{210}Ra \rightarrow {}^{4}He + {}^{206}Rn$ | 7.150 | 1.060 | 0.55 |
| $^{211}_{\Lambda}Ra \rightarrow {}^{4}He + {}^{207}_{\Lambda}Rn$ | 7.012 | 1.171 | $^{211}Ra \rightarrow {}^{4}He + {}^{207}Rn$ | 7.042 | 1.468 | |
| $^{212}_{\Lambda}Ra \rightarrow {}^{4}He + {}^{208}_{\Lambda}Rn$ | 6.902 | 1.601 | $^{212}Ra \rightarrow {}^{4}He + {}^{208}Rn$ | 7.031 | 1.493 | 1.04 |
| $^{213}_{\Lambda}Ra \rightarrow {}^{4}He + {}^{209}_{\Lambda}Rn$ | 6.888 | 1.640 | $^{213}Ra \rightarrow {}^{4}He + {}^{209}Rn$ | 6.892 | 2.164 | |
| $^{214}_{\Lambda}Ra \rightarrow {}^{4}He + {}^{210}_{\Lambda}Rn$ | 6.722 | 2.321 | $^{214}Ra \rightarrow {}^{4}He + {}^{210}Rn$ | 7.273 | 0.508 | 0.39 |
| $^{215}_{\Lambda}Ra \rightarrow {}^{4}He + {}^{211}_{\Lambda}Rn$ | 7.130 | 0.629 | $^{215}Ra \rightarrow {}^{4}He + {}^{211}Rn$ | 8.864 | −4.748 | |
| $^{216}_{\Lambda}Ra \rightarrow {}^{4}He + {}^{212}_{\Lambda}Rn$ | 8.720 | −4.761 | $^{216}Ra \rightarrow {}^{4}He + {}^{212}Rn$ | 9.525 | −6.546 | −6.74 |
| $^{217}_{\Lambda}Ra \rightarrow {}^{4}He + {}^{213}_{\Lambda}Rn$ | 9.382 | −6.601 | $^{217}Ra \rightarrow {}^{4}He + {}^{213}Rn$ | 9.161 | −5.607 | |
| $^{218}_{\Lambda}Ra \rightarrow {}^{4}He + {}^{214}_{\Lambda}Rn$ | 9.017 | −5.637 | $^{218}Ra \rightarrow {}^{4}He + {}^{214}Rn$ | 8.545 | −3.868 | −4.59 |

| | | | | | | |
|---|---|---|---|---|---|---|
| ${}^{219}_{\Lambda}Ra \rightarrow {}^{4}He + {}^{215}_{\Lambda}Rn$ | 8.403 | −3.861 | ${}^{219}Ra \rightarrow {}^{4}He + {}^{215}Rn$ | 8.138 | −2.617 | |
| ${}^{220}_{\Lambda}Ra \rightarrow {}^{4}He + {}^{216}_{\Lambda}Rn$ | 7.994 | −2.571 | ${}^{220}Ra \rightarrow {}^{4}He + {}^{216}Rn$ | 7.593 | −0.780 | −1.74 |
| ${}^{221}_{\Lambda}Ra \rightarrow {}^{4}He + {}^{217}_{\Lambda}Rn$ | 7.451 | −0.689 | ${}^{221}Ra \rightarrow {}^{4}He + {}^{217}Rn$ | 6.880 | 1.950 | |
| ${}^{222}_{\Lambda}Ra \rightarrow {}^{4}He + {}^{218}_{\Lambda}Rn$ | 6.740 | 2.111 | ${}^{222}Ra \rightarrow {}^{4}He + {}^{218}Rn$ | 6.679 | 2.785 | 1.58 |
| ${}^{223}_{\Lambda}Ra \rightarrow {}^{4}He + {}^{219}_{\Lambda}Rn$ | 6.537 | 2.982 | ${}^{223}Ra \rightarrow {}^{4}He + {}^{219}Rn$ | 5.979 | 6.057 | |
| ${}^{224}_{\Lambda}Ra \rightarrow {}^{4}He + {}^{220}_{\Lambda}Rn$ | 5.836 | 6.376 | ${}^{224}Ra \rightarrow {}^{4}He + {}^{220}Rn$ | 5.789 | 7.034 | 5.49 |
| ${}^{225}_{\Lambda}Ra \rightarrow {}^{4}He + {}^{221}_{\Lambda}Rn$ | 5.645 | 7.398 | ${}^{225}Ra \rightarrow {}^{4}He + {}^{221}Rn$ | 5.096 | 11.092 | |
| ${}^{226}_{\Lambda}Ra \rightarrow {}^{4}He + {}^{222}_{\Lambda}Rn$ | 5.019 | 11.181 | ${}^{226}Ra \rightarrow {}^{4}He + {}^{222}Rn$ | 4.871 | 12.581 | 10.70 |
| ${}^{227}_{\Lambda}Ra \rightarrow {}^{4}He + {}^{223}_{\Lambda}Rn$ | 4.727 | 13.189 | ${}^{227}Ra \rightarrow {}^{4}He + {}^{223}Rn$ | 4.365 | 16.361 | |
| ${}^{228}_{\Lambda}Ra \rightarrow {}^{4}He + {}^{224}_{\Lambda}Rn$ | 4.281 | 16.650 | ${}^{228}Ra \rightarrow {}^{4}He + {}^{224}Rn$ | 4.072 | 18.857 | |
| ${}^{229}_{\Lambda}Ra \rightarrow {}^{4}He + {}^{225}_{\Lambda}Rn$ | 3.973 | 19.367 | ${}^{229}Ra \rightarrow {}^{4}He + {}^{225}Rn$ | 3.590 | 23.620 | |
| ${}^{230}_{\Lambda}Ra \rightarrow {}^{4}He + {}^{226}_{\Lambda}Rn$ | 3.402 | 25.360 | ${}^{230}Ra \rightarrow {}^{4}He + {}^{226}Rn$ | 3.344 | 26.431 | |
| ${}^{231}_{\Lambda}Ra \rightarrow {}^{4}He + {}^{227}_{\Lambda}Rn$ | 3.242 | 27.306 | ${}^{231}Ra \rightarrow {}^{4}He + {}^{227}Rn$ | 2.905 | 32.320 | |
| ${}^{232}_{\Lambda}Ra \rightarrow {}^{4}He + {}^{228}_{\Lambda}Rn$ | 2.852 | 32.740 | ${}^{232}Ra \rightarrow {}^{4}He + {}^{228}Rn$ | 2.829 | 33.464 | |
| ${}^{233}_{\Lambda}Ra \rightarrow {}^{4}He + {}^{229}_{\Lambda}Rn$ | 2.652 | 35.973 | ${}^{233}Ra \rightarrow {}^{4}He + {}^{229}Rn$ | 2.535 | 38.411 | |
| ${}^{234}_{\Lambda}Ra \rightarrow {}^{4}He + {}^{230}_{\Lambda}Rn$ | 2.739 | 34.505 | ${}^{234}Ra \rightarrow {}^{4}He + {}^{230}Rn$ | 2.415 | 40.678 | |
| ${}^{235}_{\Lambda}Ra \rightarrow {}^{4}He + {}^{231}_{\Lambda}Rn$ | 2.432 | 39.970 | ${}^{235}Ra \rightarrow {}^{4}He + {}^{231}Rn$ | 2.325 | 42.489 | |

where $\rho_{\Lambda}(r_1)$ is the density distribution of lambda particle. The density distribution of lambda particle, $\rho_{\Lambda}(r_1)$ taken from Ref. [1, 2] and have the form

$$\rho_{\Lambda}(r) = \left(\pi b_{\Lambda}^2\right)^{-3/2} e^{-r^2/b_{\Lambda}^2} \tag{16}$$

Here $b_\Lambda = \sqrt{(4M_N + M_\Lambda)/4M_\Lambda b_\alpha}$, where $M_N$ and $M_\Lambda$ are the mass of the nucleon and $\Lambda$ particle respectively, and $b_\alpha = 1.358\,fm$. The lambda−nucleon force is short range and the strength of lambda−nucleus potential is smaller than the nucleon−nucleus potential. The potential $V_{\Lambda N}$ describes a mean field potential which a lambda particle feels inside a hyper nucleus, we have taken the mean field potential $V_{\Lambda N}$ from Ref [50] and given as,

$$V_{\Lambda N} = \frac{-V_0}{1+\exp[(r-c)/a]} \tag{17}$$

Here the constant $V_0 = 27.4\,MeV$, $a = 0.6\,fm$ and $c = 1.08A^{1/3}$. The predicted half lives ($T_{1/2} < 10^{30}$s) show that hyper $^{202-231}_{\Lambda}Ra$ nuclei are unstable against $^{4}_{\Lambda}He$ emission.

Table 2 shows the Q values for the emission of hyper $^{4}_{\Lambda}He$ from $^{202-235}_{\Lambda}Ra$. The negative Q values show that these nuclei are stable against hyper $^{4}_{\Lambda}He$ emission. Fig 1 and Fig 2 represent the plot connecting Q value and $\log_{10}(T_{1/2})$ versus neutron number of parent nuclei for the alpha decay of hyper $^{202-235}Ra$ and non−strange $^{202-235}Ra$ nuclei respectively. The peak in Q value for alpha decay from $^{216}Ra$ and hyper $^{217}_{\Lambda}Ra$ nuclei denote the role of neutron shell closure at N = 126 in daughter $^{212}Ra$ and $^{213}_{\Lambda}Rn$ daughter respectively. Also the dip (minimum) in $\log_{10}(T_{1/2})$ for alpha decay from $^{216}Ra$ and hyper $^{217}_{\Lambda}Ra$ nuclei denote the role of neutron shell closure at N=126 in the daughter nuclei.

From Fig 1 and Fig 2 it is clear that both Q value curve and alpha half lives curve of non−strange normal Ra nuclei overlap with that of hyper Ra nuclei. i.e. When the decay half lives of non−strange normal Ra nuclei are compared with that of corresponding hyper Ra nuclei with same neutron number (for e.g. half lives of $^{217}Ra$ and $^{218}_{\Lambda}Ra$ nuclei) it can be seen that the half lives do not differ much.

Fig 3 and Fig 4 represent the plot connecting Q value and $\log_{10}(T_{1/2})$ versus neutron number of parent nuclei for the $^{14}C$ cluster decay of hyper $^{202-229}_{\Lambda}Ra$ and non−strange $^{202\text{-}209}RA$ nuclei respectively. The peak in Q value and dip in $\log_{10}(T_{1/2})$ for $^{14}C$ cluster decay from $^{222}Ra$ stress the role of doubly magic $^{208}Pb$ (N =126, Z = 82) daughter in cluster decay. Also the peak in Q value and dip in $\log_{10}(T_{1/2})$ for $^{14}C$ cluster decay from hyper $^{223}_{\Lambda}Ra$ stress the role of proton and neutron shell closure (Z=82, N=126) in $^{209}_{\Lambda}Pb$ daughter.

**Table 2:** Computed Q values for the decay of hyper ${}^{4}_{\Lambda}He$ from hyper ${}^{202-235}_{\Lambda}Ra$ .

| Decay | Q Value (MeV) | Decay | Q Value (MeV) |
|---|---|---|---|
| ${}^{202}_{\Lambda}Ra \rightarrow {}^{4}_{\Lambda}He + {}^{198}Rn$ | −25.665 | ${}^{219}_{\Lambda}Ra \rightarrow {}^{4}_{\Lambda}He + {}^{215}Rn$ | −31.507 |
| ${}^{203}_{\Lambda}Ra \rightarrow {}^{4}_{\Lambda}He + {}^{199}Rn$ | −28.150 | ${}^{220}_{\Lambda}Ra \rightarrow {}^{4}_{\Lambda}He + {}^{216}Rn$ | −30.219 |
| ${}^{204}_{\Lambda}Ra \rightarrow {}^{4}_{\Lambda}He + {}^{200}Rn$ | −26.108 | ${}^{221}_{\Lambda}Ra \rightarrow {}^{4}_{\Lambda}He + {}^{217}Rn$ | −32.785 |
| ${}^{205}_{\Lambda}Ra \rightarrow {}^{4}_{\Lambda}He + {}^{201}Rn$ | −28.702 | ${}^{222}_{\Lambda}Ra \rightarrow {}^{4}_{\Lambda}He + {}^{218}Rn$ | −31.687 |
| ${}^{206}_{\Lambda}Ra \rightarrow {}^{4}_{\Lambda}He + {}^{202}Rn$ | −26.744 | ${}^{223}_{\Lambda}Ra \rightarrow {}^{4}_{\Lambda}He + {}^{219}Rn$ | −33.978 |
| ${}^{207}_{\Lambda}Ra \rightarrow {}^{4}_{\Lambda}He + {}^{203}Rn$ | −29.168 | ${}^{224}_{\Lambda}Ra \rightarrow {}^{4}_{\Lambda}He + {}^{220}Rn$ | −32.884 |
| ${}^{208}_{\Lambda}Ra \rightarrow {}^{4}_{\Lambda}He + {}^{204}Rn$ | −27.407 | ${}^{225}_{\Lambda}Ra \rightarrow {}^{4}_{\Lambda}He + {}^{221}Rn$ | −35.187 |
| ${}^{209}_{\Lambda}Ra \rightarrow {}^{4}_{\Lambda}He + {}^{205}Rn$ | −29.537 | ${}^{226}_{\Lambda}Ra \rightarrow {}^{4}_{\Lambda}He + {}^{222}Rn$ | −33.957 |
| ${}^{210}_{\Lambda}Ra \rightarrow {}^{4}_{\Lambda}He + {}^{206}Rn$ | −28.032 | ${}^{227}_{\Lambda}Ra \rightarrow {}^{4}_{\Lambda}He + {}^{223}Rn$ | −36.334 |
| ${}^{211}_{\Lambda}Ra \rightarrow {}^{4}_{\Lambda}He + {}^{207}Rn$ | −29.941 | ${}^{228}_{\Lambda}Ra \rightarrow {}^{4}_{\Lambda}He + {}^{224}Rn$ | −34.915 |
| ${}^{212}_{\Lambda}Ra \rightarrow {}^{4}_{\Lambda}He + {}^{208}Rn$ | −28.586 | ${}^{229}_{\Lambda}Ra \rightarrow {}^{4}_{\Lambda}He + {}^{225}Rn$ | −37.276 |
| ${}^{213}_{\Lambda}Ra \rightarrow {}^{4}_{\Lambda}He + {}^{209}Rn$ | −30.379 | ${}^{230}_{\Lambda}Ra \rightarrow {}^{4}_{\Lambda}He + {}^{226}Rn$ | −35.919 |
| ${}^{214}_{\Lambda}Ra \rightarrow {}^{4}_{\Lambda}He + {}^{210}Rn$ | −29.182 | ${}^{231}_{\Lambda}Ra \rightarrow {}^{4}_{\Lambda}He + {}^{227}Rn$ | −38.126 |
| ${}^{215}_{\Lambda}Ra \rightarrow {}^{4}_{\Lambda}He + {}^{211}Rn$ | −30.333 | ${}^{232}_{\Lambda}Ra \rightarrow {}^{4}_{\Lambda}He + {}^{228}Rn$ | −36.821 |
| ${}^{216}_{\Lambda}Ra \rightarrow {}^{4}_{\Lambda}He + {}^{212}Rn$ | −28.023 | ${}^{233}_{\Lambda}Ra \rightarrow {}^{4}_{\Lambda}He + {}^{229}Rn$ | −38.695 |
| ${}^{217}_{\Lambda}Ra \rightarrow {}^{4}_{\Lambda}He + {}^{213}Rn$ | −30.265 | ${}^{234}_{\Lambda}Ra \rightarrow {}^{4}_{\Lambda}He + {}^{230}Rn$ | −37.583 |
| ${}^{218}_{\Lambda}Ra \rightarrow {}^{4}_{\Lambda}He + {}^{214}Rn$ | −29.082 | ${}^{235}_{\Lambda}Ra \rightarrow {}^{4}_{\Lambda}He + {}^{231}Rn$ | −39.451 |

From Fig 3 and Fig 4 it is clear that both Q value curve and cluster decay half lives curve of non−strange normal Ra nuclei almost coincide with that of hyper Ra nuclei. i.e. when the decay half lives of non−strange normal Ra nuclei are compared with that of corresponding hyper Ra nuclei with same neutron number it can be seen that the half lives do not differ much.

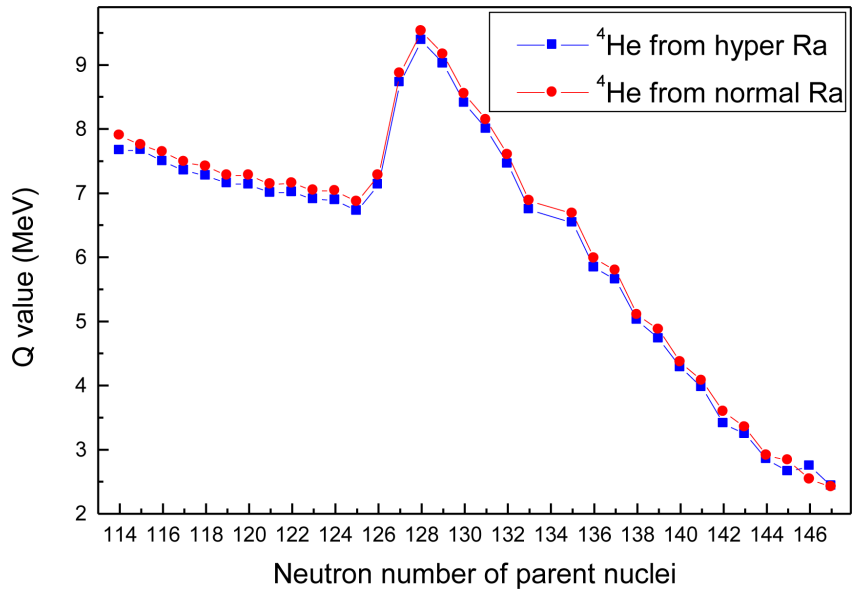


**Figure 1:** Plot connecting Q value versus neutron number for the decay of $^4He$ from hyper $^{202-235}_{\Lambda}Ra$ and non-strange $^{202\text{-}235}Ra$ nuclei.

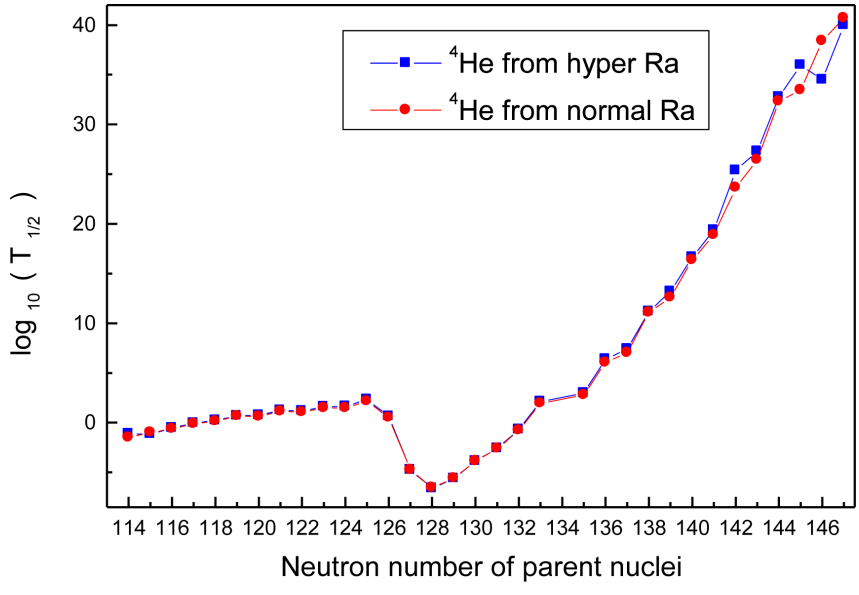


**Figure 2:** Plot connecting $\log_{10}(T_{1/2})$ versus neutron number for the decay of $^4He$ from hyper $^{202-235}_{\Lambda}Ra$ and non-strange $^{202\text{-}235}Ra$ nuclei.

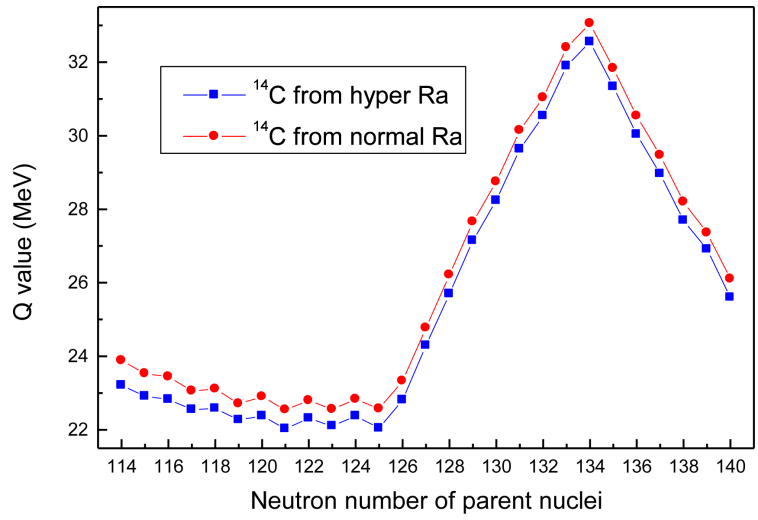


**Figure 3:**. Plot connecting Q value versus neutron number for the decay of $^{14}C$ cluster from hyper $^{202-229}_{\Lambda}Ra$ and non-strange $^{202\text{-}229}Ra$ nuclei.

Fig 5(a) and 5(b) represents the plot connecting Q value and $\log_{10}(T_{1/2})$ versus mass number of parent nuclei respectively for the $^{14}_{\Lambda}C$ cluster decay of hyper $^{202-229}_{\Lambda}Ra$ nuclei. The peak in Q value and dip (minimum) in $\log_{10}(T_{1/2})$ for $^{14}_{\Lambda}C$ cluster decay from hyper $^{222}_{\Lambda}Ra$ indicate the role of doubly magic $^{208}Pb$ daughter in the decay. The computed half life for hyper $^{14}_{\Lambda}C$ emission from hyper $^{202-229}_{\Lambda}Ra$ nuclei is found to have large values, $T_{1/2} > 10^{66}$s which shows that hyper $^{217-229}_{\Lambda}Ra$ nuclei are stable against hyper $^{14}_{\Lambda}C$ emission.

In Table 3 the computed Q values and $\log_{10}(T_{1/2})$ values for the $^{14}C$ cluster emission from hyper $^{202-229}_{\Lambda}Ra$ and non−strange $^{202\text{-}229}Ra$ are given. The predicted $^{14}C$ decay half life for $^{217-229}_{\Lambda}Ra$ are well within the present upper limit for measurement ($T_{1/2} < 10^{30}$s) and these decays are favorable for measurement.

We have compared the computed logarithm of alpha half lives for normal Ra isotopes with experimental data [51] given in the last column of Table 1. The computed values are in agreement with experimental data and the standard deviation of logarithm of computed alpha half is found to be 1.01. The standard deviation is computed using the relation

$$\sigma = \sqrt{\frac{1}{(n-1)}\sum_{i=1}^{n}\left[\log\left(T_{1/2}^{cal.}\right) - \log\left(T_{1/2}^{\exp.}\right)\right]^2} \qquad (18)$$

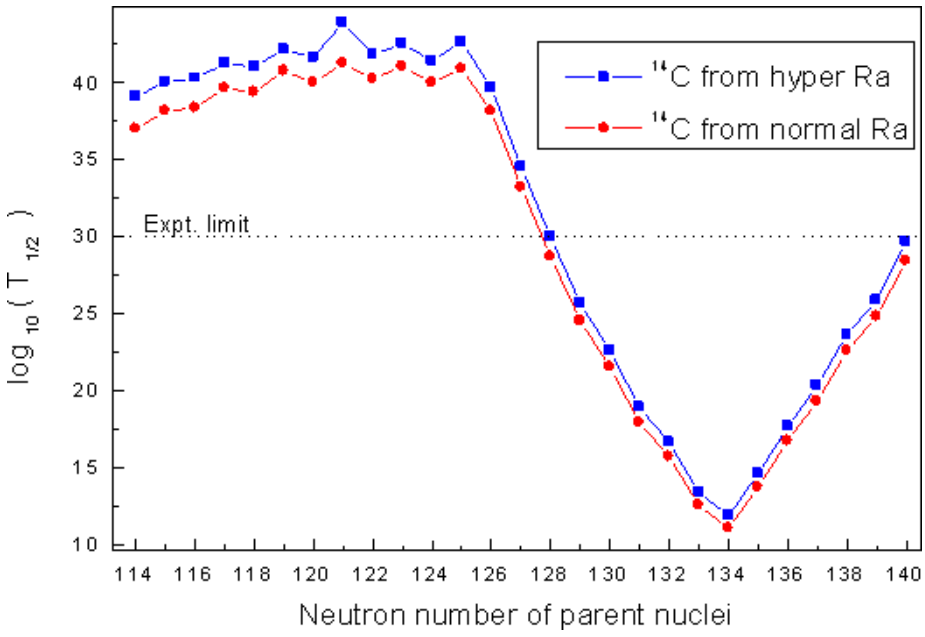


**Figure 4:** Plot connecting $\log_{10}(T_{1/2})$ versus neutron number for the decay of $^{14}C$ cluster from hyper $^{202-229}_{\Lambda}Ra$ and non-strange $^{202-229}Ra$ nuclei.

We have also compared the half lives for $^{14}$C emission from various normal Ra isotopes with experimental values. From Table 2 it is clear that the computed $\log_{10}(T_{1/2})$ values for $^{14}$C emission from normal Ra isotopes are in good agreement with experimental values [52].

## SUMMARY

The possibilities of alpha and $^{14}C$ cluster emission from hyper $^{202-235}Ra$ nuclei are studied using the Coulomb and Proximity Potential Model (CPPM) by including the lambda−nucleus potential. The Q values are calculated using the recent mass tables of Wang et al [48]. The predicted half lives show that hyper $^{202-231}_{\Lambda}Ra$ nuclei are unstable against $^{4}He$ emission and $^{14}C$ emission from $^{217-229}_{\Lambda}Ra$ are favorable for measurement. Our study also show that hyper $^{202-235}_{\Lambda}Ra$ are stable against hyper $^{4}_{\Lambda}He$ and $^{14}_{\Lambda}C$ emission. The role of neutron shell closure (N=126) in $^{213}_{\Lambda}Rn$ daughter and role of proton/ neutron shell closure (Z=82, N=126) in $^{209}_{\Lambda}Pb$ daughter are also revealed. The computed alpha and $^{14}C$ cluster half lives from normal Ra nuclei are compared with corresponding experimental data and are found to be in good agreement. As hyper nuclei decays to normal nuclei

**Table 3**: Computed Q value and logarithm of half lives for the decay of $^{14}C$ from hyper $^{202-229}_{\Lambda}Ra$ and non−strange $^{202\text{-}229}Ra$ nuclei. $T_{1/2}$ is in second.

| Decay | Q Value (MeV) | $\log_{10}(T_{1/2})$ | Decay | Q Value (MeV) | $\log_{10}(T_{1/2})$ | |
|---|---|---|---|---|---|---|
| | | | | | Theory | Expt [52] |
| $^{202}_{\Lambda}Ra \rightarrow {}^{14}C + {}^{188}_{\Lambda}Pb$ | 23.210 | 39.145 | $^{202}Ra \rightarrow {}^{14}C + {}^{188}Pb$ | 23.886 | 37.003 | |
| $^{203}_{\Lambda}Ra \rightarrow {}^{14}C + {}^{189}_{\Lambda}Pb$ | 23.211 | 39.067 | $^{203}Ra \rightarrow {}^{14}C + {}^{189}Pb$ | 23.530 | 38.148 | |
| $^{204}_{\Lambda}Ra \rightarrow {}^{14}C + {}^{190}_{\Lambda}Pb$ | 22.912 | 40.060 | $^{204}Ra \rightarrow {}^{14}C + {}^{190}Pb$ | 23.443 | 38.378 | |
| $^{205}_{\Lambda}Ra \rightarrow {}^{14}C + {}^{191}_{\Lambda}Pb$ | 22.830 | 40.284 | $^{205}Ra \rightarrow {}^{14}C + {}^{191}Pb$ | 23.060 | 39.654 | |
| $^{206}_{\Lambda}Ra \rightarrow {}^{14}C + {}^{192}_{\Lambda}Pb$ | 22.550 | 41.236 | $^{206}Ra \rightarrow {}^{14}C + {}^{192}Pb$ | 23.111 | 39.406 | |
| $^{207}_{\Lambda}Ra \rightarrow {}^{14}C + {}^{193}_{\Lambda}Pb$ | 22.580 | 41.058 | $^{207}Ra \rightarrow {}^{14}C + {}^{193}Pb$ | 22.710 | 40.781 | |
| $^{208}_{\Lambda}Ra \rightarrow {}^{14}C + {}^{194}_{\Lambda}Pb$ | 22.270 | 42.142 | $^{208}Ra \rightarrow {}^{14}C + {}^{194}Pb$ | 22.902 | 40.020 | |
| $^{209}_{\Lambda}Ra \rightarrow {}^{14}C + {}^{195}_{\Lambda}Pb$ | 22.380 | 41.665 | $^{209}Ra \rightarrow {}^{14}C + {}^{195}Pb$ | 22.543 | 41.262 | |
| $^{210}_{\Lambda}Ra \rightarrow {}^{14}C + {}^{196}_{\Lambda}Pb$ | 22.030 | 42.919 | $^{210}Ra \rightarrow {}^{14}C + {}^{196}Pb$ | 22.801 | 40.256 | |
| $^{211}_{\Lambda}Ra \rightarrow {}^{14}C + {}^{197}_{\Lambda}Pb$ | 22.310 | 41.800 | $^{211}Ra \rightarrow {}^{14}C + {}^{197}Pb$ | 22.561 | 41.071 | |
| $^{212}_{\Lambda}Ra \rightarrow {}^{14}C + {}^{198}_{\Lambda}Pb$ | 22.100 | 42.529 | $^{212}Ra \rightarrow {}^{14}C + {}^{198}Pb$ | 22.831 | 40.025 | |
| $^{213}_{\Lambda}Ra \rightarrow {}^{14}C + {}^{199}_{\Lambda}Pb$ | 22.375 | 41.435 | $^{213}Ra \rightarrow {}^{14}C + {}^{199}Pb$ | 22.570 | 40.917 | |
| $^{214}_{\Lambda}Ra \rightarrow {}^{14}C + {}^{200}_{\Lambda}Pb$ | 22.040 | 42.639 | $^{214}Ra \rightarrow {}^{14}C + {}^{200}Pb$ | 23.324 | 38.150 | |
| $^{215}_{\Lambda}Ra \rightarrow {}^{14}C + {}^{201}_{\Lambda}Pb$ | 22.814 | 39.705 | $^{215}Ra \rightarrow {}^{14}C + {}^{201}Pb$ | 24.773 | 33.221 | |
| $^{216}_{\Lambda}Ra \rightarrow {}^{14}C + {}^{202}_{\Lambda}Pb$ | 24.292 | 34.526 | $^{216}Ra \rightarrow {}^{14}C + {}^{202}Pb$ | 26.211 | 28.713 | |
| $^{217}_{\Lambda}Ra \rightarrow {}^{14}C + {}^{203}_{\Lambda}Pb$ | 25.701 | 29.982 | $^{217}Ra \rightarrow {}^{14}C + {}^{203}Pb$ | 27.654 | 24.521 | |
| $^{218}_{\Lambda}Ra \rightarrow {}^{14}C + {}^{204}_{\Lambda}Pb$ | 27.150 | 25.657 | $^{218}Ra \rightarrow {}^{14}C + {}^{204}Pb$ | 28.741 | 21.542 | |
| $^{219}_{\Lambda}Ra \rightarrow {}^{14}C + {}^{205}_{\Lambda}Pb$ | 28.235 | 22.609 | $^{219}Ra \rightarrow {}^{14}C + {}^{205}Pb$ | 30.145 | 17.930 | |
| $^{220}_{\Lambda}Ra \rightarrow {}^{14}C + {}^{206}_{\Lambda}Pb$ | 29.638 | 18.910 | $^{220}Ra \rightarrow {}^{14}C + {}^{206}Pb$ | 31.036 | 15.733 | |

| | | | | | | | |
|---|---|---|---|---|---|---|---|
| ${}^{221}_{\Lambda}Ra \rightarrow {}^{14}C + {}^{207}_{\Lambda}Pb$ | 30.536 | 16.646 | ${}^{221}Ra \rightarrow {}^{14}C + {}^{207}Pb$ | 32.396 | 12.565 | 13.39 |
| ${}^{222}_{\Lambda}Ra \rightarrow {}^{14}C + {}^{208}_{\Lambda}Pb$ | 31.898 | 13.403 | ${}^{222}Ra \rightarrow {}^{14}C + {}^{208}Pb$ | 33.050 | 11.076 | 11.01 |
| ${}^{223}_{\Lambda}Ra \rightarrow {}^{14}C + {}^{209}_{\Lambda}Pb$ | 32.549 | 11.891 | ${}^{223}Ra \rightarrow {}^{14}C + {}^{209}Pb$ | 31.829 | 13.740 | 15.20 |
| ${}^{224}_{\Lambda}Ra \rightarrow {}^{14}C + {}^{210}_{\Lambda}Pb$ | 31.334 | 14.601 | ${}^{224}Ra \rightarrow {}^{14}C + {}^{210}Pb$ | 30.535 | 16.725 | 15.68 |
| ${}^{225}_{\Lambda}Ra \rightarrow {}^{14}C + {}^{211}_{\Lambda}Pb$ | 30.037 | 17.663 | ${}^{225}Ra \rightarrow {}^{14}C + {}^{211}Pb$ | 29.466 | 19.318 | |
| ${}^{226}_{\Lambda}Ra \rightarrow {}^{14}C + {}^{212}_{\Lambda}Pb$ | 28.960 | 20.341 | ${}^{226}Ra \rightarrow {}^{14}C + {}^{212}Pb$ | 28.197 | 22.583 | 21.19 |
| ${}^{227}_{\Lambda}Ra \rightarrow {}^{14}C + {}^{213}_{\Lambda}Pb$ | 27.694 | 23.683 | ${}^{227}Ra \rightarrow {}^{14}C + {}^{213}Pb$ | 27.362 | 24.831 | |
| ${}^{228}_{\Lambda}Ra \rightarrow {}^{14}C + {}^{214}_{\Lambda}Pb$ | 26.909 | 25.848 | ${}^{228}Ra \rightarrow {}^{14}C + {}^{214}Pb$ | 26.103 | 28.436 | |
| ${}^{229}_{\Lambda}Ra \rightarrow {}^{14}C + {}^{215}_{\Lambda}Pb$ | 25.599 | 29.701 | ${}^{229}Ra \rightarrow {}^{14}C + {}^{215}Pb$ | 25.109 | 31.452 | |

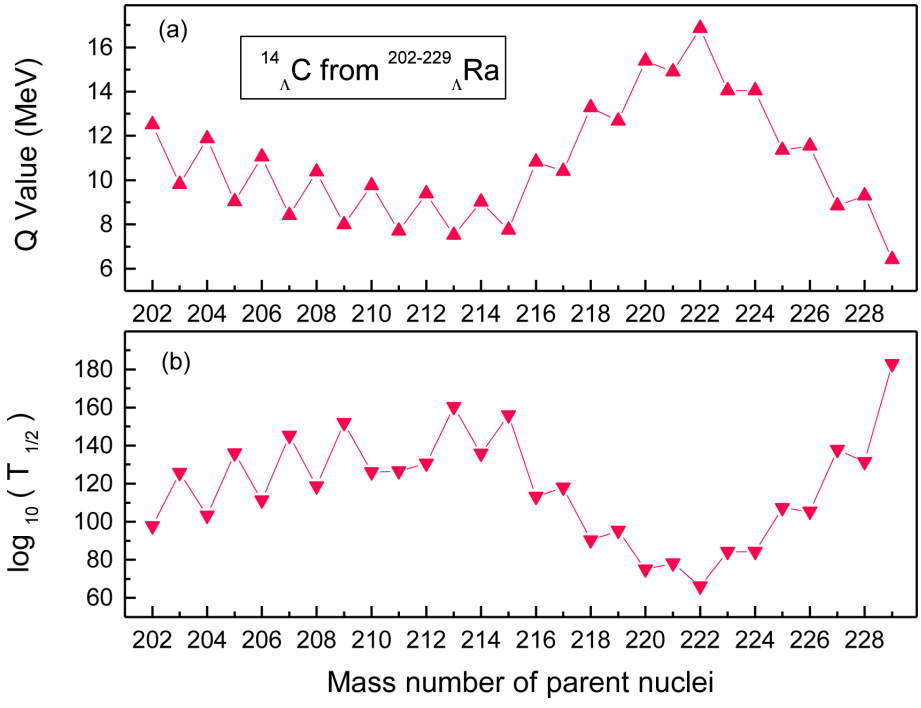


**Figure 5:** Plot connecting (a) Q value versus mass number and (b) $\log_{10}(T_{1/2})$ versus. mass number for the decay of hyper ${}^{14}_{\Lambda}C$ cluster from hyper ${}^{202-229}_{\Lambda}Ra$ nuclei.

by mesonic/non−mesonic decay and since most of the predicted half lives for $^{4}He$ and $^{14}C$ emission from normal Ra nuclei are favorable for measurement, we presume that alpha and $^{14}C$ cluster emission from hyper Ra nuclei can be detected in laboratory in a cascade (two−step) process.

## REFERENCES

[1] T. Motoba, H. Bando and K. Ikeda, Prog. Theor. Phys. **70**, 189 (1983).
[2] K. Hagino and T. Koike, Phys. Rev. C **84**, 064325 (2011).
[3] E. Hiyama, M. Kamimura, Y. Yamamoto, T. Motoba, and T.A. Rijken, Prog. Theo. Phys. Suppl. **185**, 106 (2010).
[4] M.T. Win, K. Hagino and T. Koike, Phys. Rev. C **83**, 014301 (2011).
[5] J.M. Yao, Z.P. Li, K. Hagino, M.T.Win, Y. Zhang and J. Meng, Nucl. Phys. A **868**, 12 (2011).
[6] D. Vretenar, W. Poschl, G.A. Lalazissis and P. Ring, Phys. Rev. C **57**, 1060 (1998).
[7] X. R. Zhou, A. Polls, H. J. Schulze, and I. Vidana, Phys. Rev. C **78**, 054306 (2008).
[8] C. Samanta, P. R. Chowdhury and D. N. Basu, J. Phys. G: Nucl. Part. Phys. **35**, 065101 (2008).
[9] Minato, S. Chiba, and K. Hagino, Nucl. Phys. A **831**, 150 (2009).
[10] F. Minato and S. Chiba, Nucl. Phys. A **856**, 55 (2011).
[11] H. Ohm, T. Hermes, W. Borgs, H. R. Koch, R. Maier, D. Prasuhn, H. J. Stein, O. W. B Schult, K. Pysz, Z. Rudy, L. Jarczyk, B. Kamys, P. Kulessa, A. Strzalkowski, W. Cassing, Y. Uozumi and I. Zychor I 1997 Phys. Rev. C **55**, 3062 (1997).
[12] M. Danysz, J. Pniewski, Philos. Mag. **44**, 348 (1953).
[13] O. Hashimoto and H. Tamura, Prog. Part.and Nucl. Phys. **57**, 564 (2006).
[14] F. Cusanno et al, Phys. Rev. Lett. **103**, 202501 (2009).
[15] M. Iodice et al, Phys. Rev. Lett. **99**, 052501(2007).
[16] A. Cieply, E. Friedman, A. Gal and V. Krejcirik, Phys. Lett. B **698**, 226 (2011).
[17] E. Rutherford and H. Geiger, Proc. R. Soc. **81**, 162 (1908).
[18] E. Rutherford and T. Royds, Phil. Mag. **17**, 281 (1909).
[19] G. Gamow, Z. Phys. **51**, 204 (1928).
[20] R. W. Gurney and E. U. Condon, Nature (London) **122**, 439 (1928).
[21] J. Dong, H. Zhang, Y. Wang, W. Zuo and J. Li, Nucl. Phys. A **832**, 198 (2010).
[22] D. Ni and R. Zhong−zhou, J. Phys. G: Nucl. Part. Phys. **37**, 035104 (2010).
[23] V. Yu. Denisov and A. A. Khudenko, Phys. Rev. C **80**, 034603 (2009).
[24] K. P. Santhosh and A. Joseph, Ind. J. Pure & Appl. Phys. **42**, 806 (2004).
[25] A. Sandulescu, D. N. Poenaru and W. Greiner, Sov. J. Part. Nucl. **11**, 528 (1980).

[26] H. J. Rose and G. A. Jones, Nature **307**, 245 (1984).

[27] D. N. Poenaru, M. Ivascu, A. Sandulescu and W. Greiner, J. Phys. G: Nucl. Part. Phys. **10**, 183 (1984).

[28] G. A. Pik−Pichak, Sov. J. Nucl. Phys. **44,** 923 (1986).

[29] G. Shanmugam and B. Kamalaharan, Phys. Rev. C **38,** 1377 (1988).

[30] K. P. Santhosh, Pramana − J. Phys. **76**, 431 (2011).

[31] M. Iriondo, D. Jerrestan and R. J. Liotta, Nucl. Phys. A **454,** 252 (1986).

[32] R. Blendoaske, T. Fliessbach and H. Walliser, Nucl. Phys. A **464,** 75 (1987).

[33] S. S. Malik and R. K. Gupta, Phys. Rev. C **39**, 1992 (1989).

[34] K. P. Santhosh, Eur. Phys. J. A **49**, 127 (2013).

[35] Y. J. Shi and W. J. Swiatecki, Nucl. Phys. A **438**, 450 (1985).

[36] I. Dutt and R. K. Puri, Phys. Rev. C **81**, 064608 (2010).

[37] I. Dutt and R. K. Puri, Phys. Rev. C **81**, 064609 (2010).

[38] Y. J. Shi and W. J. Swiatecki, Nucl. Phys. A **464**, 205 (1987).

[39] J. Blocki, J. Randrup, W. J. Swiatecki and C. F. Tsang, Ann. Phys. (NY) **105**, 427 (1977).

[40] J. Blocki and W. J. Swiatecki, Ann. Phys. (NY) **132**, 53 (1981).

[41] D. N. Poenaru, M. Ivascu, A. Sandulescu and W. Greiner, Phys. Rev. **C 32**, 572 (1985).

[42] H. Bando, T. Motoba and J. Zofka, Int. J. Mod. Phys. A **5**, 4021 (1990).

[43] L. Majling, Nucl. Phys. A **585**, 211 (1995).

[44] P. H. Pile, S. Bart, R. E. Chrien, D. J. Millener, R. J. Sutter, N. Tsoupas, J.−C. Peng, C. S. Mishra, E. V. Hungerford, T. Kishimoto, L.−G. Tang, W. von Witsch, Z. Xu, K. Maeda, D. Gill, R. McCrady, B. Quinn, J. Seydoux, J. W. Sleight, R. L. Stearns, H. Plendl, A. Rafatian, and J. Reidy, Phys. Rev. Lett. **66**, 2585 (1991).

[45] G. A. Lalazissis, M. E. Grypeos and S. E. Massen, Phys. Rev. C **37**, 2098 (1988).

[46] G. A. Lalazissis, Phys. Rev. C **49**, 1412 (1994).

[47] T. Hasegawa, O. Hashimoto, S. Homma, T. Miyachi, T. Nagae, M. Sekimoto, T. Shibata, H. Sakaguchi, T. Takahashi, K. Aoki, H. Noumi, H. Bhang, M. Youn, Y. Gavrilov, S. Ajimura, T. Kishimoto, A. Ohkusu, K. Maeda, R. Sawafta, and R. P. Redwine, Phys. Rev. C **53**, 1210 (1996).

[48] M. Wang, G. Audi, A.H. Wapstra, F.G. Kondev, M. MacCormick, X. Xu, and B. Pfeiffer, Chinese Phys. C **36**, 1603 (2012).

[49] C. Samanta, P. R. Chowdhury and D. N. Basu, J Phys G: Nucl Part Phys **32**, 363 (2006).

[50] P. B. Siegel and M. Farrow Reid, Am. J. Phys. **58**, 1016 (1990).

[51] NuDat2.5, http://www.nndc.bnl.gov.

[52] R. Bonetti and A. Guglielmetti, Rom. Rep. Phys. **59**, 301 (2007).